ARTICLE

Conformations of Carnosine in Aqueous Solutions by All-Atom Molecular Dynamics Simulations and 2D-NOSEY Spectrum

Rong Zhang*, Dan Wang, Wen-juan Wu

Laboratory of Physical Chemistry, College of Pharmacy, Guangdong Pharmaceutical University, Guangzhou 510006, China

(Dated: Received on December 4, 2012; Accepted on January 8, 2013)

All-atom molecular simulations and two-dimensional nuclear overhauser effect spectrum have been used to study the conformations of carnosine in aqueous solution. Intramolecular distances, root-mean-square deviation, radius of gyration, and solvent-accessible surface are used to characterize the properties of the carnosine. Carnosine can shift between extended and folded states, but exists mostly in extended state in water. Its preference for extension in pure water has been proven by the 2D nuclear magnetic resonance (NMR) experiment. The NMR experimental results are consistent with the molecular dynamics simulations.

Key words: All-atom molecular simulation, Carnosine aqueous solution, Two-dimensional nuclear overhauser effect spectrum

I. INTRODUCTION

Carnosine is a dipeptide of β-alanine and L-histidine in skeletal muscle. This compound is a radical scavenger and a possible neurotransmitter-like molecule that regulates neuronal functions [1−8]. In the pharmaceutical industry, carnosine is found in relatively high concentrations in several body tissues. It is also used as an anti-aging agent, thus is called the fountain of youth [9, 10]. Carnosine can inhibit oxidation under pH and temperature conditions expected during the processing and storage of muscle food [11]. The carnosine molecule contains imidazole, a five-membered heterocyclic ring that is important in biological activities. The behavior of imidazole under pressure in carnosine can provide new reaction mechanisms, which can lead to novel material synthesis [12, 13]. Murli *et al.* used Raman spectroscopy to study the ring-opening polymerization in carnosine under pressure [13]. The onset of ring-opening polymerization involving the imidazole ring occurs at pressures of approximately 2.8 GPa. A substantial fraction of the monomer is converted to a polymer network at pressures above 12 GPa. Hipkiss investigated the anti-aging actions of carnosine. Carnosine was found to exert anti-convulsant effects in rodents [14]. The dipeptide is speculated to participate in the repair of protein isoaspartyl groups. Molecular dynamics (MD) simulation has been proven to be particularly valuable for the research on the structures and interactions in biomolecular systems [15−17]. Spectral measurements such as nuclear magnetic resonance (NMR) spectra are highly powerful techniques, which can be used to investigate interactions and structures of biochemical molecules in solutions [18−20]. We previously investigated the interactions and the structures in a special associated system such as amide-water and small peptide mixtures [21−24]. Several interesting phenomena were observed in the mixture, such as weak C−H$\cdots$O contacts and excess properties.

Although several theories and experiments have been adopted to study carnosine, the hydrogen-bonding network and correlative conformation of carnosine in aqueous solution have seldom been explored using two-dimensional (2D) NMR and MD simulations. To gain a deeper insight into the carnosine-water system, radial distribution functions (RDFs), intramolecular distance (Dis), radius of gyration, root-mean-square deviation (RMSD), and information on the 2D nuclear Overhauser effect spectroscopy (NOESY) spectrum were used to reveal the interactions in carnosine aqueous solutions.

II. COMPUTATIONAL METHODS

A. Molecular models

Simple rigid models were used for both water and carnosine. The nonbonded interactions are denoted by a sum of Coulomb and Lennard-Jones terms in Eq.(1).

$$E_{\rm ab} = \sum_{i}^{\rm ona}\sum_{j}^{\rm onb}\left[q_i q_j \frac{{\rm e}^2}{r_{ij}} + 4\varepsilon_{ij}\left(\frac{\sigma_{ij}^{12}}{r_{ij}^{12}} - \frac{\sigma_{ij}^{6}}{r_{ij}^{6}}\right)\right] f_{ij} \quad (1)$$

where $E_{\rm ab}$ is interaction energy between two molecules a and b. q is partial charge on atom. ε and σ are the

*Author to whom correspondence should be addressed. E-mail: zhangr_zju@hotmail.com, FAX: +86-20-39352129

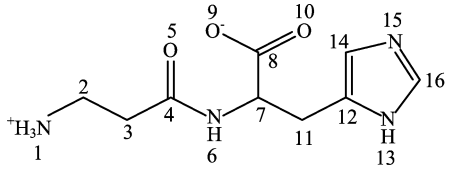

FIG. 1 Structure of carnosine molecule.

well depth parameter and collision diameter in Lennard-Jones functions, respectively. r denotes the distance between two atoms. Standard combination rules were used via Eq.(2) and Eq.(3).

$$\sigma_{ij} = (\sigma_{ii}\sigma_{jj})^{1/2} \tag{2}$$

$$\varepsilon_{ij} = (\varepsilon_{ii}\varepsilon_{jj})^{1/2} \tag{3}$$

The same expression is used for intramolecular non-bonded interactions between all the pairs of atoms (i<j) separated by three or more bonds. In Eq.(1), f_{ij} equals 1.0 except for intramolecular 1,4 interactions with f_{ij}=0.5.

The simple point charge (SPC) model [25, 26] and the optimized potentials for liquid simulation-all atom (OPLS-AA) model [27, 28] were used for water and carnosine molecules, respectively. The carnosine molecule is ionized in aqueous solution and maintains the charged state in the neutral solution. The structure of carnosine is illustrated in Fig.1. Potential parameters and symbol of the atoms for SPC water and carnosine are shown in Table I.

TABLE I Potential parameters and symbol of the atoms for SPC water and carnosine.

Atom	σ/Å	ε/(kJ/mol)	q/e
SPC			
OW	3.1410	0.1554	−0.8068
HW	0.0000	0.0000	0.4034
Carnosine			
N1	3.2500	0.1700	−0.3000
H1(NH_3)	0.0000	0.0000	0.3300
C2	3.5000	0.0660	0.1900
H2	2.5000	0.0300	0.0600
C3	3.5000	0.0660	−0.1200
H3	2.5000	0.0300	0.0600
C4	3.7500	0.1050	0.5000
O5	2.9600	0.2100	−0.5000
N6(N−H)	3.2500	0.1700	−0.5000
H6	0.0000	0.0000	0.3000
C7	3.5000	0.0660	0.0400
H7	2.5000	0.0300	0.0600
C8	3.7500	0.1050	0.7000
O9	2.9600	0.2100	−0.8000
O10(COO^-)	2.9600	0.2100	−0.8000
C11	3.5000	0.0660	−0.0050
H11	2.5000	0.0300	0.0600
C12	3.5500	0.0700	0.2150
N13	3.2500	0.1700	−0.5400
H13	0.0000	0.0000	0.4600
C14	3.5500	0.0700	0.2150
H14	2.4200	0.0300	0.1150
N15	3.2500	0.1700	−0.5400
H15	0.0000	0.0000	0.4600
C16	3.5500	0.0700	0.3850
H16	2.4200	0.0300	0.1150

B. Simulation details

MD calculations were performed using a modified TINKER 5.1 molecular modeling package [29]. The simulations were carried out in the NPT ensemble at T=298 K and P=101 kPa. The carnosine molecule was placed in a cubic box and solvated by 512 SPC water molecules to study the conformations in the dilute solutions. Periodic boundary conditions were adopted with a spheric cutoff. The particle-mesh Ewald (PME) method was used for long-range electrostatics. Energies of the initial configurations were minimized by the MINIMIZE program in the TINKER 5.1 package. Simulations of 5 ns were used for equilibrium, and simulations of 20 ns were used for analysis. Configurations were saved every 1 ps. The initial conformation was obtained from the beginning conformation of the molecule in MD simulations.

C. Definitions

The radius of gyration ($R_{\rm g}$) is defined as follows [30]

$$R_{\rm g} = \sqrt{\sum_{i=1}^{N} \frac{(r_i - r_g)^2}{N}} \tag{4}$$

where r_g represents the position of the molecular center, r_i represents the position of the i atom, and N is the number of the atoms. Solvent-accessible surface areas (ASAs) of carnosine were calculated using the Connolly algorithm [31]. The RMSD of each atom in carnosine from the initial conformation was also calculated. The distance is defined between terminal NH_3^+ and CO_2^-.

III. EXPERIMENTS

^{1}H-NMR, ^{1}H-^{1}H COSY, and 2D-NOESY spectra were measured using a Bruker DMX 500 spectrometer operating at 500 MHz with an accuracy of ±0.1 °C. The mixing time was 80 ms, and the number of scans was set to 16. The carnosine exiguous solution (0.05 mol/L) consisted of 90%H_2O-10%D_2O, which is used in biological NMR [32, 33]. The ^{1}H NMR at different temperatures of 298, 308, 318, and 328 K were

DOI:10.1063/1674-0068/26/01/67-72

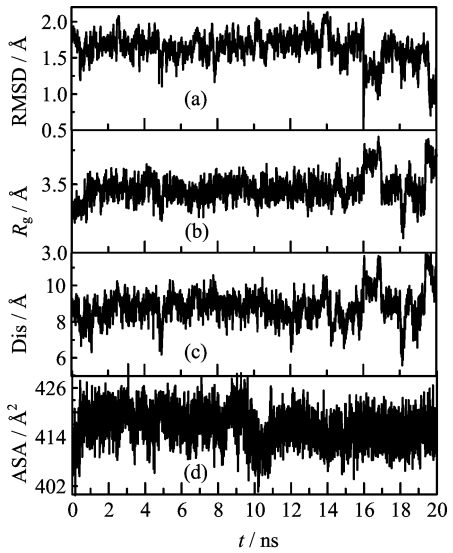

FIG. 2 The variety of the properties in carnosine aqueous solution with time dependence in simulation. (a) RMSD, (b) R_g, (c) distance between terminal NH_3^+ and CO_2^-, and (d) accessible surface area.

also measured.

IV. RESULTS AND DISCUSSION

A. Conformational analysis

The Dis, R_g, RMSDs, and ASA are four of the most important factors to be considered when analyzing the flexibility and the conformation of biomolecules in a solution. The simulations are characterized in terms of these four factors, as shown in Fig.2. The variations in the four characteristic properties show consistency with time dependence. The shorter the intramolecular distance between terminal NH_3^+ and CO_2^-, the more folded the conformations will be. The values of R_g and surface area decrease because of the folded conformation. The folded conformation of carnosine deviates from the initial structures, which also results in increased RMSD.

The carnosine states can be classified by the distribution of the square of R_g^2 [34]. The distribution of R_g^2 in the 20 ns simulations is shown in Fig.3. The folded state can be classified as the range of R_g^2<10.5 Å^2. The extended state can be classified as the range of R_g^2>13 Å^2, and R_g^2 of the semifolded state is between 10.5 and 13 Å^2. Carnosine mainly prefers the extended and the semifolded conformations, and the folded conformation is not often observed. The distances between the terminal NH_3^+ and CO_2^- (Fig.2) ranges from 8 Å to 10 Å, which can also be classified as the extended conformation region. The carnosine molecule is highly flexible in aqueous solution, as shown by RMSD, R_g, distance, and surface area as functions of simulation time. The carnosine molecule does not exist as a unique native state and can convert quickly from extended to folded conformations. The carnosine molecule mainly prefers the extended conformation.

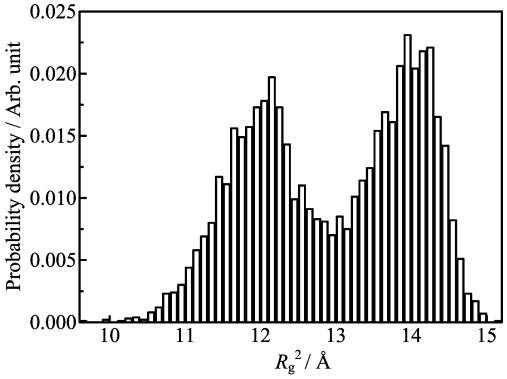

FIG. 3 The probability distribution of R_g^2 in carnosine aqueous solutions.

B. RDF and hydrogen bond analysis

The structure of a liquid is well characterized by RDF. The RDFs for hydrogen atoms (H13 and H6) in different NH groups and water molecules are illustrated in Fig.4(a). The different hydrogen atoms in the NH groups show different capabilities and stabilities in forming N−H···O hydrogen bonds. H13 is the hydrogen atom in the imidazole ring. The first peak in $g(r)$[OW−H13] is remarkably higher than that in $g(r)$[OW−H6]. The distance of the first peak in $g(r)$[OW−H13] (approximately 1.7 Å) is shorter than that in $g(r)$[OW−H6] (approximately 1.9 Å). These results indicate that the amide hydrogen atom in the imidazole ring is more favored in forming strong hydrogen bonds of N−H···O than the amide hydrogen atom in the carbon chain. The RDFs for different weak C−H···O contacts are also demonstrated in Fig.4(b). The intensity of $g(r)$[OW−H16] is stronger and the distance is shorter than those of $g(r)$[OW−H7]. These results reveal that the hydrogen atoms of the methyl group in the imidazole ring are more favored in forming weak C−H···O contacts than those hydrogen atoms in the carbon chain. The weak C−H···O contacts can not be neglected in the mixtures although the intensities of the weak C−H···O contacts are weaker than those of the strong hydrogen bonds. The first broad peaks of the RDFs also indicate that the intermolecular interactions are likely to include weak hydrogen bonds and other weak interactions, such as dipolar interactions and dispersions.

For further insight into the carnosine-water mixtures, several typical clusters of carnosine generated by a trajectory analysis of the simulations are depicted in Fig.5. The water molecules preferably form hydrogen bonds with the amide hydrogen atom in the imidazole ring than that in the carbon chain. Different

DOI:10.1063/1674-0068/26/01/67-72

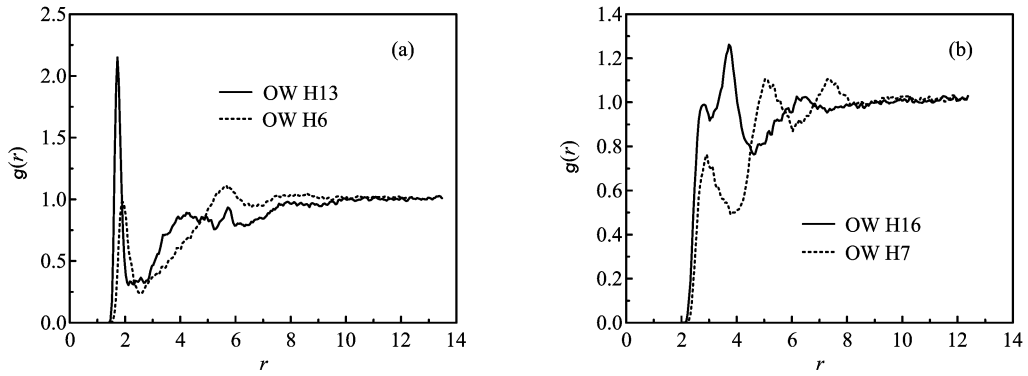

FIG. 4 The radial distribution function in simulation. (a) $g(r)$ of the hydrogen atom in amide and oxygen atom in water. (b) $g(r)$ of the hydrogen atom in methyl group and oxygen atom in water. The symbols are shown in Table I.

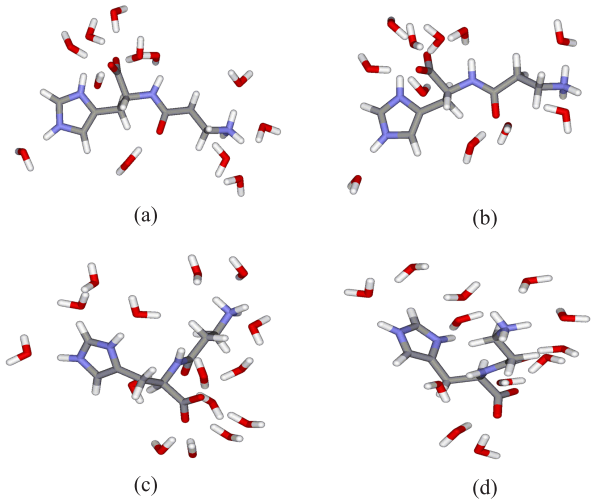

FIG. 5 Typical clusters of carnosine in aqueous solutions. all amide hydrogen atoms can form N−H···OW hydrogen bonds with water in the extended conformation ((a) and (b)) and in the folded conformation ((c) and (d)).

cases are observed in different conformational states of carnosine. For example, in the extended conformation (Fig.5 (a) and (b)), all amide hydrogen atoms can form N−H···OW hydrogen bonds with water. However, in the folded conformation (Fig.5 (c) and (d)), hydrogen bonds are preferably formed between water and amide hydrogen atoms in the imidazole ring, which show agreement with the RDFs in MD simulations.

C. Comparison to NMR experiments

NMR spectroscopy is frequently used to investigate intermolecular interactions of biomolecules in solution. Efficient NMR-based structural determination relies on the measurement of nuclear overhauser effects, which yield ^{1}H-^{1}H upper distance limit constraints [35, 36]. ^{1}H NMR, ^{1}H-^{1}H COSY, and 2D-NOESY were measured in the present work. The chemical shifts of the

TABLE II Chemical shifts of different hydrogen atoms of carnosine in aqueous solution at 298 K.

Atom type	δ/ppm	Atom type	δ/ppm
H16	7.5963	H11	3.0106
H14	6.8289	H11	2.8502
H7	4.3401	H3	2.5345
H2	3.0983	HW	4.7017

different hydrogen atoms of carnosine in aqueous solution are classified according to the ^{1}H-^{1}H COSY results shown in Table II. The NOESY spectrum of carnosine in aqueous solution is illustrated in Fig.6. The findings from MD simulations show good agreement with the NOESY spectra obtained.

Hydrogen bond interactions are sensitive to temperature variations. A strong hydrogen bond leads to a larger shift than a weak hydrogen bond. The shift of the water hydrogen (HW) atom is obvious. However, for the methyl hydrogen atom, no obvious change is observed with temperature. The variations of the relative chemical shifts with temperature which also reflect the capabilities of forming hydrogen bonds. The chemical shifts of different temperature-dependent hydrogen atoms are shown in Table III. The changes in the HW atoms with the temperature ($\Delta\delta/\Delta T \approx 11\times10^{-3}$ ppm/K) are considerably larger than those of methyl hydrogen atoms ($\Delta\delta/\Delta T \approx 0.2\times10^{-3}$ ppm/K to 0.5×10^{-3} ppm/K). These results reveal that the hydrogen bonds of OW−HW···OW are markedly stronger than those weak C−H···O contacts.

NOESY spectra provide information about protons which are 5 Å or less apart in space, not bonds. The presence of a NOE peak is a direct evidence that two protons are within 5 Å from each other in space. In aqueous solution, HW atoms show several weak NOE signals relative to the hydrogen atoms in carnosine (peaks 1, 4, 7, and 8). However, for the intramolecular interaction of carnosine, the H2 atoms (peak 4 in Fig.6) show weak NOE signals relative to the H3 atoms (peak

DOI:10.1063/1674-0068/26/01/67-72

TABLE III Temperature-dependent chemical shifts of different hydrogen atoms in carnonsine aqueous solution.

T/K	H16	H14	H7	H2	H11	H11	H3	HW
298	7.5963	6.8289	4.3401	3.0983	3.0106	2.8502	2.5345	4.7017
308	7.5986	6.8296	4.3396	3.1017	3.0146	2.8520	2.5343	4.5858
318	7.6030	6.8307	4.3390	3.1055	3.0186	2.8542	2.5343	4.4738
328	7.6075	6.8321	–	3.1098	3.0230	2.8570	2.5345	4.3714
$(\Delta\delta/\Delta T)/(10^{-3}$ ppm/K)	0.3733	0.1067	0.0550	0.3833	0.4133	0.2267	0.0100	11.0100

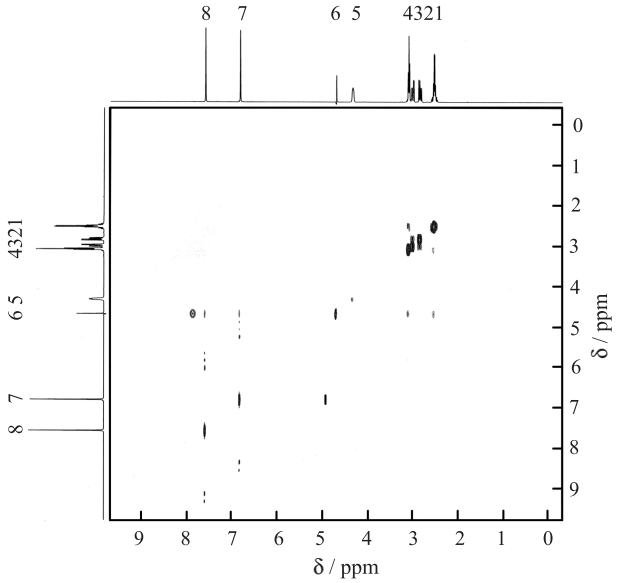

FIG. 6 NOESY spectrum of carnosine in aqueous solutions. Peaks 1 to 8 denote the chemical shifts of the different hydrogen atoms of carnosine in aqueous solutions: 1. H3, 2. H11, 3. H11, 4. H2, 5. H7, 6. HW, 7. H14, 8. H16.

1 in Fig.6). The H2 and the H3 atoms are close to each other in carnosine. No other signal is found between two atoms in carnosine. The results of the 2D NOESY spectrum reveal that carnosine exists in the extended state in aqueous solution, which show good agreement with the MD simulations.

D. Role of water

MD simulations and 2D NOESY spectra show that carnosine is mostly in the extended state in aqueous solutions. The simulations exhibit that carnosine is highly flexible in aqueous solution. The conformations can be converted from extended to folded. Numerous biomolecules are active only in aqueous solution. Water molecules show highly strong capability in forming hydrogen bonds, and can form bridge hydrogen bonds with carnosine to make the cluster more stable. As a good proton acceptor and donor, water can easily break the folded conformation. The competition-forming hydrogen-bonding interactions of carnosine in aqueous solution lead to the hydrogen bond networks and the distribution conformations, which affect the carnosine activity under physiological conditions.

V. CONCLUSION

The conformations and the structures in carnosine-water system were examined by the all-atom MD simulations and 2D NOESY spectra. Dis, R_g, RMSD, and ASA were calculated to examine the conformational flexibility of carnosine in aqueous solutions. Simulations revealed that carnosine does not exist in a unique native state, but exists mostly in extended state in water. This phenomenon was proven by the 2D NOESY spectrum. The NMR experimental results are consistent with the MD simulations. The variation in the distribution of conformations and the hydrogen-bonding network has an important function under physiological conditions.

VI. ACKNOWLEDGMENTS

This work was supported by the National Natural Science Foundation of China (No.20903026), the Talents Introduction Foundation for Universities of Guangdong Province (2011), and the Scientific Research Foundation of the Natural Science Foundation of Guangdong Province, China (No.S2011010002483).

[1] S. Tsai, W. Kuo, W. Liu, and M. Yin, J. Agric. Food Chem. **58**, 11510 (2010).
[2] C. Suer, N. Dolu, A. S. Artis, L. Sahin, and S. Aydogan, Neuropeptides **45**, 77 (2011).
[3] H. Otani, A. Okumura, K. Nagai, and N. Okumura, Neurosci. Lett. **445**, 166 (2008).
[4] P. J. Quinn, A. A. Boldyrev, and V. E. Formazuyk, Mol. Aspects Med. **13**, 379 (1992).
[5] Y. Horii, J. Shen, Y. Fujisaki, K. Yoshida, and K. Nagai, Neurosci. Lett. **510**, 1 (2012).
[6] L. Mora, M. A. Sentandreu, and F. Toldraa, J. Agric. Food Chem. **55**, 4664 (2007).
[7] L. Bonfanti, P. Peretto, S. De. Marchis, and A. Fasolo, Neurobiol. **59**, 333 (1999).
[8] D. G. Ririe, P. R. Roberts, M. N. Shouse, and G. P. Zaloga, Nutrition **16**, 168 (2000).

DOI:10.1063/1674-0068/26/01/67-72

[9] M. Ohsawa, J. Mutoh, M. Asato, S. Yamamoto, H. Ono, H. Hisa, and J. Kamei, Eur. J. Pharmaco. **682**, 56 (2012).
[10] M. Mong, C. Chao, and M. Yin, Eur. J. Pharmaco. **653**, 82 (2011).
[11] E. A. Decker, A. D. Crum, and J. T. Calvert, J. Agric. Food Chem. **40**, 756 (1992).
[12] D. Chelazzi, M. Ceppatelli, M. Santoro, R. Bini, and V. Schettino, Nat. Mater. **3**, 470 (2004).
[13] C. Murli, A. K. Mishra, S. Thomas, and S. M. Sharma, J. Phys. Chem. B **116**, 4671 (2012).
[14] A. R. Hipkiss, Exp. Gerontol. **44**, 237 (2009).
[15] A. Khalfa and M. Tarek, J. Phys. Chem. B **114**, 2676 (2010).
[16] B. A. Hall and M. S. P. Sansom, J. Chem. Theory Comput. **5**, 2465 (2009).
[17] M. Wang, J.Yang, J. Wang, and X. Wang, Chin. J. Chem. **30**, 24 (2012).
[18] M. G. Reddy and N. S. Caldarelli, Anal. Chem. **82**, 3266 (2010).
[19] J. Griffiths, Anal. Chem. **81**, 1725 (2009).
[20] K. Mizuno, S. Imafuji, T. Fujiwara, T. Ohta, and Y. Tamiya, J. Phys. Chem. B **107**, 3972 (2003).
[21] R. Zhang, D. Zheng, Y. Pan, S. Luo, and H. Li, J. Mol. Struct. **875**, 96 (2008).
[22] R. Zhang, H. Li, Y. Lei, and S. Han, J. Phys. Chem. B **109**, 7482 (2005).
[23] R. Zhang, W. Zeng, X. Meng, J. Huang, and W. Wu, Chem. Phys. **402**, 130 (2012).
[24] R. Zhang and W. Wu, J. Mol. Liq. **162**, 20 (2012).
[25] P. Mark and L. Nilsson, J. Phys. Chem. A **105**, 9954 (2001).
[26] D. C. Berweger, W. F. Gunsteren, and F. Müller-Plathe, Chem. Phys. Lett. **232**, 429 (1995).
[27] D. S. Maxwell and J. Tirado-Rives, J. Am. Chem. Soc. **118**, 11225 (1996).
[28] W. L. Jorgensen and C. Swenson, J. Am. Chem. Soc. **107**, 1489 (1985).
[29] M. J. Dudek, K. Ramnarayan, and J. W. Ponder, J. Comput. Chem. **19**, 548 (1998).
[30] A. Luzar and D. Chandler, J. Chem. Phys. **98**, 8160 (1993).
[31] M. L. Connolly, J. Appl. Crystallogr. **16**, 548 (1983).
[32] G. Zheng, T. Stait-Gardner, P. G. Kumar, A. M. Torres, and W. S. Price, J. Magn. Reson. **191**, 159 (2008).
[33] R. P. L. Clairac, B. H. Geierstanger, M. Mrksich, P. B. Dervan, and D. E. Wemmer. J. Am. Chem. Soc. **119**, 7909 (1997).
[34] Y. Lei, H. Li, R. Zhang, and S. Han, J. Phys. Chem. B **108**, 10131 (2004).
[35] S. Raman, Y. J. Huang, B. Mao, P. Rossi, J. M. Aramini, G. Liu, G. T. Montelione, and D. Baker, J. Am. Chem. Soc. **132**, 202 (2010).
[36] B. D. Ray, J. Scott, H. Yan, and B. D. N. Rao, Biochemistry **48**, 5532 (2009).

DOI:10.1063/1674-0068/26/01/67-72